β^+–Delayed-Proton Decay of ^{21}Mg†

Richard G. Sextro, R. A. Gough, and Joseph Cerny
Department of Chemistry and Lawrence Berkeley Laboratory, University of California, Berkeley, California 94720
(Received 5 March 1973)

Identified protons with energies from 900 keV to 6.3 MeV have been observed following the positron decay of ^{21}Mg. The half-life of ^{21}Mg was measured to be 123.1 ± 3.3 msec, which, combined with previous results, gives a best value of 122.5 ± 2.8 msec. The energies and intensities of the proton groups have been used to determine precise excited state energies in ^{21}Na above 5 MeV and the strength of the preceding β^+ transition feeding each level. These data, and the assumption of isospin purity for the lowest $T = \frac{3}{2}$ level in ^{21}Na, then yield absolute ft values for the beta decay. The ^{21}Mg transition rates compared with the negatron decay rates in its mirror, ^{21}F, give $(ft)^+/(ft)^- = 1.10 \pm 0.08$. All significant particle decays of the lowest $T = \frac{3}{2}$ level have been observed, including an upper limit on energetically possible, but unobserved, α decay. The measured transition strengths were compared to recent shell model calculations for β decay in the s–d shell.

I. INTRODUCTION

The nuclide ^{21}Mg is one of the series of $T_z = -\frac{3}{2}$, $A = 4n + 1$, β^+–delayed-proton precursors. These nuclei have substantial positron decay branches to particle-unbound levels in their daughters. The energies and intensities of the particle groups resulting from breakup of the unbound levels can be used to determine excitation energies of states in the β^+-decay daughter nucleus and the transition strengths feeding these levels. If these *relative* transition rates can be related to absolute decay rates to the daughter, measurement of the particle decays will yield absolute ft values for the preceding β^+ decay.[1] This method permits the accurate determination of β-decay rates spanning several orders of magnitude.

Shell-model predictions of excitation energies and β-decay transition rates have been recently calculated by Lanford and Wildenthal[2] for nuclei in the *sd* shell, employing for mass 21 a *complete sd* basis space for the five nucleons outside an ^{16}O core. Experimental measurements of ft values for transitions arising in the decay of ^{21}Mg permit a new and sensitive test of these wave functions, which in general have been reasonably successful in describing energy spectra, spectroscopic factors for single-nucleon transfer reactions, and electromagnetic observables.[2]

Moreover, β-decay studies in mass 21 can furnish additional information on the question of mirror β-decay asymmetry. The original review of mirror β-decay transition rates in light nuclei by Wilkinson[3] points out an apparent proportionality relating the discrepancy between these rates and the $\beta^\pm$-decay energy given by

$$\delta \equiv \frac{(ft)^+}{(ft)^-} - 1 \propto W_0^+ + W_0^- , \tag{1}$$

where the superscripts + and – refer to positron and negatron decay, respectively, and W_0 is the total decay energy. From this observed proportionality to the decay energies, a value of $\delta \cong 0.07$ can be obtained for mass 21. However, an analysis of ^{21}Mg vs ^{21}F β decays employing the earlier delayed-proton data from McGill[4] shows strong disagreement with this prediction. More recent work by Wilkinson and others[5] on the β decay of $T_z = \pm 1$ isobars indicates that the systematic evidence for a "fundamental" mirror asymmetry between even-A isobars has in fact largely disappeared in light of new experimental data, though the odd-mass systems continue to show significant positive values for δ (though not necessarily of nontrivial origin[5]). It is of some interest to examine mass 21 also in this context.

Although ^{21}Mg has been previously investigated,[4] the earlier experiments were hampered by a large, low-energy background, relatively poor resolution, and a limited observable energy range. The present experiments utilized a counter telescope and particle identifier in conjunction with a helium-jet transport system[6] to produce high-quality, low-background particle spectra. These measurements cover a broad energy range, spanning all the significant particle decays of those excited levels in ^{21}Na fed by the positron decay of ^{21}Mg.

II. EXPERIMENTAL TECHNIQUE

The external beam of the Berkeley 88-in. cyclotron was used to initiate the ^{20}Ne(^{3}He, $2n$)^{21}Mg reaction. A bombarding energy of 29.5 MeV, which is substantially above the 22.0-MeV threshold[7] for producing ^{21}Mg, was chosen to avoid the possibility of producing ^{17}Ne via the ^{20}Ne(^{3}He, $\alpha 2n$) reaction whose threshold is 31.2 MeV. This bombarding energy is also sufficient to produce ^{20}Na [via

^{20}Ne(^{3}He, $p2n$)]. However, ^{20}Na ($T_{1/2}$ = 446 msec[8]) is a β^+-delayed-α precursor and has no known β^+-decay branch to proton-unbound levels; although protons could arise from the decay of ^{20}Ne levels fed by electron capture in ^{20}Na, the *maximum* possible proton energy in the center of mass would be $\leq$1.05 MeV.

In order to minimize the background and obtain high-resolution proton spectra, a helium-jet system was developed for the transport of activity away from the target area and beam. A schematic diagram of this system is shown in Fig. 1. The cyclotron beam, typically 3 μA, enters through a 5.6-μm Havar foil window located 5.2 cm from the target position. The beam exits through a similar foil window and is refocused into a Faraday cup located ~1.8 m downstream. For these experiments the target chamber was pressurized to ~1200 Torr (absolute) of commercial spark chamber gas consisting of 90% neon and 10% helium. (For this particular case the sweeping gas also served as a target gas. In other experiments, targets were placed on the wheel shown in Fig. 1 and helium was used as a sweeping gas.) A portion of the ^{21}Mg recoils produced by the ^{3}He beam was thermalized within the 2.5-cm-long collector cylinder (cross-hatched in Fig. 1). These recoils were entrained in the gas flow and swept into the 0.48-mm-i.d. capillary tube. This stainless-steel tube carried the recoil nuclei and gas a distance of 40 cm and directed the flow against a collector foil positioned 3 mm from the end of the capillary.

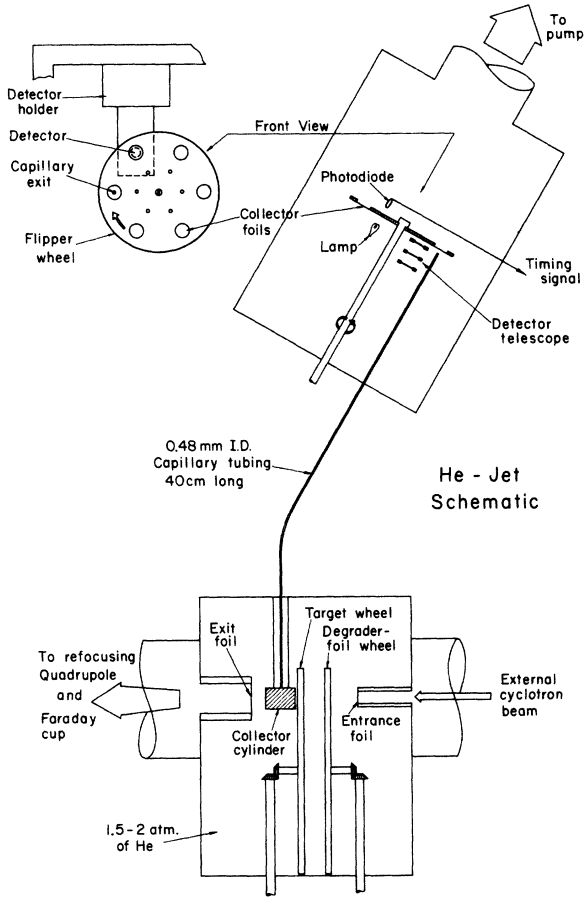

FIG. 1. A simplified drawing of the helium-jet transport system. Details of its use are given in the text.

This collection/counting chamber was continuously pumped on by a 45-liter/sec Roots-blower-mechanical-pump combination and was maintained at a pressure of ~0.3 Torr. The flow through the capillary tube was measured to be ~16 Torr liter/sec. The collector consisted of a 10-cm-diam aluminum wheel with six collection foils mounted 60° apart. Typically these foils were 50-μm-thick aluminum disks.

A remotely controlled solenoidal stepping motor moved the foils from the collection position to the counting position; this position change required approximately 25 msec. Although the stepping motor could be fired as often as 10 times per second, for these experiments a rate of two steps per second was used (for a cycle time of 500 msec). No pulsing of the beam was required with this arrangement; thus while one foil was positioned in front of the capillary tube, the adjacent foil was being counted.

Several different ΔE-E detector combinations were used in the course of these experiments in order to span a broad energy range. The ΔE detector ranged in thickness from 4 to 50 μm, while the E detector was 50, 265, or 500 μm thick. Each ΔE-E telescope was followed by a 100-μm, 1.5-cm-diam reject detector which was operated in anticoincidence with the first two detectors to eliminate signals from protons traversing them. The solid angle of 0.24 sr subtended by the counter telescopes was limited in every case by the diameter of the E counter. All detectors were cooled to -25° C, except the very thin ΔE detectors.

The signals from the ΔE and E detectors and associated electronics were sent to a Goulding-Landis particle identifier[9] after having met a coincidence requirement of $2\tau \sim 40$ nsec. Normally only those events corresponding to protons were recorded, thereby eliminating all α particles following the β decay of ^{20}Na. However, in searching for possible low-energy α particles from the decay of highly excited states *in* ^{21}Na, both proton and α groups were identified and their associated energy signals were recorded separately.

The electronic energy resolution was dependent upon the exact combination of detectors, but ranged from 25 to 45 keV full width at half maxi-

mum (FWHM). This resolution was influenced by the large capacitance of the very thin ΔE detectors. The observed proton widths were also affected by momentum broadening due to the preceding β^+ decay and, in some cases, by the intrinsic widths of broad states themselves. Generally, very low backgrounds were observed, though a small background contribution arising from multiply scattered β particles was recorded in the lower-energy portion of the spectrum obtained with the thickest telescope (50-μm ΔE and 500-μm E).

The collector wheel provided a timing signal used to initiate each counting cycle. Small holes in the aluminum wheel were located on the same radial axes as the collector foils. A light beam passed through the hole onto a photodiode. This beam was interrupted when the collector wheel was stepped by the solenoidal motor. The "on" signal was reestablished by the light beam and photodiode when the wheel stopped moving; this signal, suitably delayed ~30 msec to allow wheel-induced pickup to die away, gated the analyzers on for the predetermined counting period (usually 400 msec) and initialized the time sequence used for storing lifetime information.

Half-life data were acquired in two ways. The total energy signals (E_T) were stored in a Nuclear Data 4096-channel analyzer, operating in an 8 $\times$512-channel mode. The eight groups corresponded to sequential time segments each typically 50 msec long; thus eight-point half-life information could be obtained for each statistically-significant peak in the energy spectrum. For the second method, logic signals corresponding to a peak of interest in the E_T spectrum were recorded using a 400-channel analyzer operating in the multiscale mode. A quartz-crystal oscillator advanced the channel address at a preset rate.

III. EXPERIMENTAL RESULTS

A. Energy Calibration

The lowest $T=\frac{3}{2}$ states in ^{21}Na and ^{25}Al exhibit significant proton decay branches to both the ground and first excited states in their respective decay daughters, ^{20}Ne and ^{24}Mg. Excitation energies of these analog states have been accurately measured by resonance scattering,[10,11] resonance capture,[12] and particle-transfer reactions.[13] The energies of their prominent proton decays $-E_{\rm lab}$ $\simeq$4.09 and 5.40 MeV for ^{25}Al, and $\simeq$4.67 and 6.23 MeV for ^{21}Na – can therefore be used as calibration points for the high-energy portion of the ^{21}Na proton spectrum ($E_{\rm lab}$~ 2 to 7 MeV). As part of this calibration, the delayed-proton precursor ^{25}Si was produced by the ^{24}Mg(^{3}He, $2n$)^{25}Si reaction at 29.5 MeV and the recoils collected using helium as a sweeping gas.

As a check on the accuracy of a variety of measurements of $T=\frac{3}{2}$ levels in $T_z=-\frac{1}{2}$, $A=4n+1$ nuclei, the delayed-proton precursors ^{21}Mg, ^{25}Si, ^{29}S, and ^{37}Ca were studied in a separate experiment.[14] The observed proton decay energies from the lowest $T=\frac{3}{2}$ levels were fitted with a straight line via least squares. All were found to be internally consistent, within errors, giving assurance of the accuracy of the chosen calibrants.

The low-energy proton spectra were calibrated as follows. Accurate resonance energies, corresponding to states at E_x~ 3.55, 4.29, and 4.47 MeV in ^{21}Na have been measured,[15,16] as have γ transitions from these levels.[16,17] A weighted average of these values gives proton decay energies (lab) of 1.060 $\pm$ 0.0004, 1.773 $\pm$ 0.002, and 1.939 $\pm$ 0.005 MeV, respectively. These energies were then used in conjunction with the $T=\frac{3}{2}$ decay data to establish a calibration for the spectrum acquired using the 11-μm ΔE, 265-μm E telescope ($E_{\rm lab}$~ 700 keV to 5.5 MeV). For data taken with a 6-μm ΔE, the three low-energy points alone served as calibrants.

B. Proton Spectra

An identified proton spectrum obtained with an 11-μm ΔE and 265-μm E detector telescope is shown in Fig. 2. The energy region between 2.4 and 7.5 MeV, taken with 50-μm ΔE and 500-μm E counters, is shown in Fig. 3, with better statistics than in Fig. 2. The numbers above the peaks correspond to the peak numbers and decay assignments in Table I. Additional data, not shown here, were acquired with a 6-μm ΔE and 50-μm E tele-

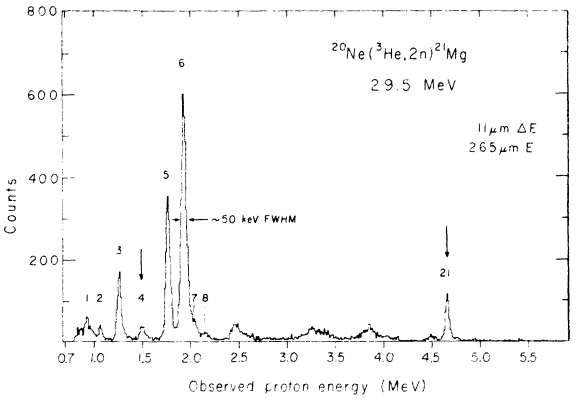

FIG. 2. An identified-proton spectrum acquired with the counter telescope noted in the figure. All peaks are associated with the decay of ^{21}Mg and are numbered to correspond with the data listed in Table I. The vertical arrows denote decays from the $T=\frac{3}{2}$ state in ^{21}Na.

scope, spanning the energy range from ~0.7 to 2.2 MeV. It is difficult to estimate an absolute cross section for the production of ^{21}Mg via this technique; however, our approximate proton yield was 0.08 events per μC of beam.

No known β^+–delayed-proton precursors could be produced from likely contaminants in the target gas. The proton spectra obtained consist solely of breakup of levels in ^{21}Na. As further evidence for this, the half-lives for all statistically significant peaks in the sequential time-routed data were found to be consistent with the parent ^{21}Mg half-life.

Between 2.5 and 4.5 MeV, the spectra are composed primarily of three sets of multiple peaks, making the extraction of accurate intensities difficult. Figure 4 shows a typical decomposition of one set of multiple peaks using a Gaussian peak-fitting program. The energies, intensities, and widths of peaks 9 through 19 remained consistent

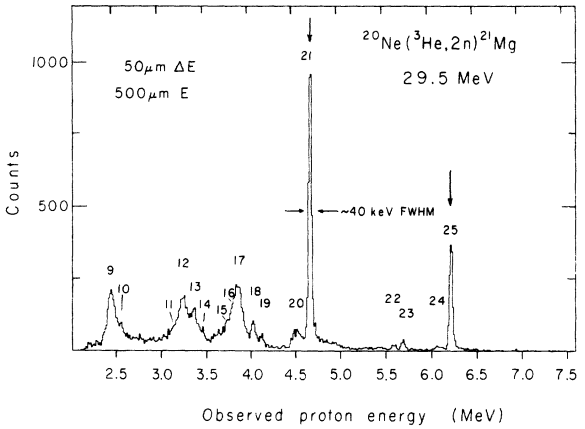

FIG. 3. Delayed protons from ^{21}Mg with energies greater than 2.4 MeV. Again the numbers correspond to proton decay data shown in Table I; the vertical arrows point to peaks arising from the $T=\frac{3}{2}$ state decay.

TABLE I. Proton energies from the decay of unbound levels in ^{21}Na fed by β^+ decay of ^{21}Mg, and a comparison of ^{21}Na energy levels inferred from this work with previous results. Underlined numbers preceding each entry correspond to peak-identification numbers shown in Figs. 2 and 3. (All entries given as MeV ± keV.)

Proton energies (c.m.) corresponding to decay to the following levels in ^{20}Ne:				Deduced[a] energies in	Previous work		
g.s.	1.634 MeV	4.247 MeV	4.968 MeV	^{21}Na	Ref. 22	Ref. 20	Other
2 1.113 ± 0.4[b]				3.545 ± 2	3.544 ± 8	3.54 ± 20	
5 1.862 ± 2[b]	...[c]			4.294 ± 3	4.294 ± 9	4.28 ± 30	
6 2.036 ± 5[b]	...			4.468 ± 5	4.468 ± 9	4.41 ± 30	
9 2.598 ± 20	1 0.947 ± 20			5.022 ± 15	4.99 ± 50	4.99 ± 30	5.03[d]
X	3 1.320 ± 10			5.386 ± 10		5.34 ± 30	
11 3.326 ± 35	X[c]			5.758 ± 35	5.69	5.78 ± 30	
12 3.435 ± 25	X			5.867 ± 25	5.82		
13 3.547 ± 15	X[e]			5.979 ± 15			
14 3.662 ± 35	X[e]			6.094 ± 35	6.08		
15 3.78 ± 50	X[e]			6.21 ± 50	6.24	6.16 ± 30	
16 3.930 ± 35	8 2.265 ± 25			6.341 ± 20			
17 4.068 ± 20	X			6.500 ± 20	6.51	6.54 ± 30	6.52[f]
22 5.865 ± 15	18 4.246 ± 25	X	X	8.301 ± 15	(8.35)	8.31 ± 30	
23 5.986 ± 15	19 4.350 ± 20	X	X	8.417 ± 15			
24 6.387 ± 25	20 4.741 ± 15	7 2.145 ± 15	X [g]	8.816 ± 10			
25 6.538 ± 4[b]	21 4.904 ± 4[b]	X	4 1.573 ± 10 [g]	8.970 ± 4[h]	8.90 ± 40	8.97 ± 30[i]	
Unassigned proton peak: 10 2.718 ± 30[j]							

[a] The energies are calculated using a proton separation energy of 2.432 ± 0.002 MeV, which represents an average of values determined in Refs. 7, 16, and 17.

[b] These proton energies were used, in part, to determine the energy calibration (see discussion in Sec. III A of the text).

[c] Unobserved, but energetically allowed, proton decays within our experimental range are marked by X, while those outside our range (≤700 keV) are shown by ···.

[d] M. Amiel, M. Lambert, and H. Beaumevieille, Lettere Nuovo Cimento 1, 689 (1969).

[e] These possible decays were obscured by peaks arising from the decay of other states.

[f] P. Bém, J. Habanec, O. Karban, and J. Němec, Nucl. Phys. A96, 529 (1967).

[g] Possible proton decays from these levels leading to higher excited states in ^{20}Ne are also within our energy range, but no such decays were observed.

[h] This number is based on the average of the delayed-proton results and resonance measurements discussed in Ref. 14.

[i] This number is corrected based on the remeasured mass of ^{10}C [H. Brunnader, J. C. Hardy, and J. Cerny, Phys. Rev. 174, 1247 (1968)].

[j] The possible origin of this peak is discussed in the text.

over three separate experiments when analyzed in this manner.

The experimental energy resolution is indicated in Figs. 2 and 3 for the counter telescopes used. Typically, momentum broadening from the preceding β^+ decay contributed 5–14 keV to this width.

C. α-Particle Spectrum and Results

States in ^{21}Na above 6.56 MeV excitation are unbound to α decay to ^{17}F (as can be noted from the ^{21}Mg decay scheme shown in Fig. 6 below). In particular, the lowest $T=\frac{3}{2}$ state is α unbound by 2.4 MeV.[7] Simple barrier-penetrability predictions for $l=0$ α emission from the ^{21}Na $T=\frac{3}{2}$ level to the ^{17}F ground state suggest that, as an upper limit, this (isospin-forbidden) decay is relatively unhindered by the Coulomb barrier. (In fact, the penetrability for this α decay is comparable to that calculated for the proton decay of the analog state to the third excited state in ^{20}Ne, as shown in Table III below.)

An experimental search for this possible decay mode used a counter telescope consisting of a 4-μm ΔE detector, a 48-μm E detector and a 100-μm reject detector. α particles as low as 1.4 MeV could be reliably identified. The resulting spectrum is shown in Fig. 5; as can be seen, the β^+-delayed-α decay of ^{20}Na dominates the spectrum. Since proton data were collected simultaneously, direct comparison of the intensities establishes a limit for this possible decay branch of <1.6% relative to the total proton decay.

The energy scale was taken from the known decays of the 7.42- and 10.26-MeV levels[18] in ^{20}Ne, which result in α energies (lab) of 2.16 and 4.42 MeV, respectively. Using these as calibrants, the energies of the other major peaks arising from ^{20}Na decay are shown in Fig. 5. The intensities of these peaks relative to the 2.16-MeV peak (100%) are: (2.50) 4.5%; (3.81) 1.8%; (4.42) 17.8%; (4.66) 0.6%; (4.86) 1.3%. These values agree with the recent results[19] on ^{20}Na.

D. Half-Life Measurements

The use of counter telescopes and particle identification reduced the background to a negligible level. In addition, ^{21}Mg was the only known delayed-proton precursor present in the spectra. Hence no systematic errors from contaminant activity should be present to distort the measured lifetimes. Combining data acquired using the two methods described earlier in Sec. II, our determination of the ^{21}Mg half-life, resulting from four independent experiments, is 123.1 ± 3.3 msec. This compares well with the previously reported ^{21}Mg half-life of 121 ± 5 msec[4] and results in a weighted average of 122.5 ± 2.8 msec. This average value has been used for all subsequent calculations and results quoted in this paper.

IV. ANALYSIS

A. Energies and Intensities

The center-of-mass proton energy and the parent state in ^{21}Na for each of the analyzed peaks

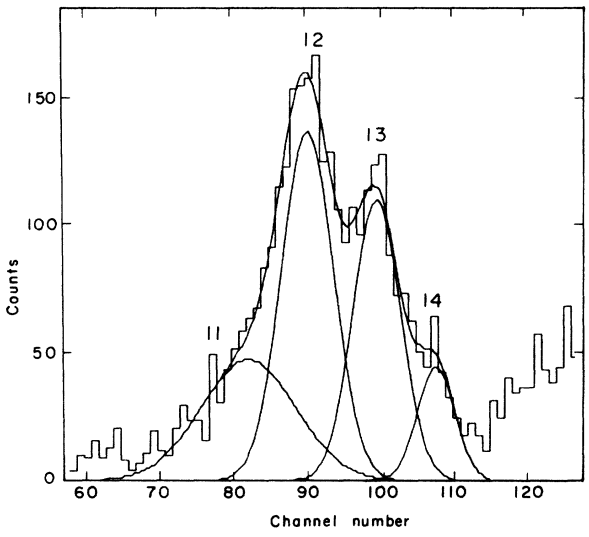

FIG. 4. A sample multiple-peak group between 3.0 and 3.5 MeV analyzed using a Gaussian peak-fitting program (see discussion in text). The numbering system and data are identical to that in Fig. 3.

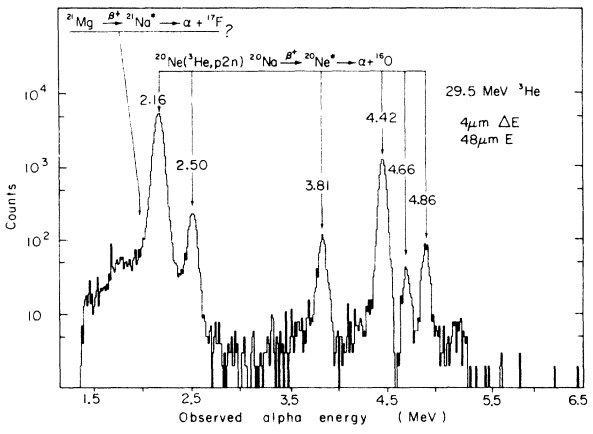

FIG. 5. Identified α-particle spectrum following ^{3}He bombardment of ^{20}Ne. The predicted location for the α particles from decay of the ^{21}Na $T=\frac{3}{2}$ state is shown by the arrow at lowest energy. The remaining arrows indicate α particles and their respective energies (lab) in MeV following the β^+ decay of ^{20}Na.

are shown in Table I. The observed proton energies are averages over several different experiments and ΔE-E detector combinations. Unfortunately, some ambiguities remain regarding a few of the assignments for the observed proton decays. These arise due to the two or more decay modes available to states above ~5 MeV. The ground-state spin and parity of ^{21}Mg is presumed to be $\frac{5}{2}^+$, analogous to the $\frac{5}{2}^+$ ground state in its mirror, ^{21}F. Further verification for this comes from the determination that the spin and parity for the lowest $T=\frac{3}{2}$ state in each of the $T_z=\pm\frac{1}{2}$ isobars is $\frac{5}{2}^+$ (^{21}Ne: Ref. 20; ^{21}Na: Ref. 21). Therefore the states in ^{21}Na populated by allowed β decay will have $J^\pi=\frac{3}{2}^+$, $\frac{5}{2}^+$, or $\frac{7}{2}^+$.

The energy levels of ^{21}Na up to ~5 MeV have been extensively studied,[16,22] most recently by Haas, Johnson, and Bair[17] using ^{20}Ne(p,γ) and

TABLE II. Branching ratios and ft values for the positron decay of ^{21}Mg.

Energy level[a] in ^{21}Na (MeV)	J^π[b]	Proportion of proton decays[c] (%)	Branching ratio[d] from ^{21}Mg (%)	ft[d,e] (10^3 sec)	Logft (sec)	Theoretical predictions[f] Logft (sec)	E_x in ^{21}Na (MeV)	J^π
0.000	$\frac{3}{2}^+$		15.8±4.0[g]	182±46	5.26±0.10	5.55	0.000	$\frac{3}{2}^+$
0.332	$\frac{5}{2}^+$		40.7±5.0[g]	62±8	4.79±0.05	4.70	0.314	$\frac{5}{2}^+$
1.723	$\frac{7}{2}^+$		10.9±2.0[g]	126±23	5.10±0.07	4.80	1.800	$\frac{7}{2}^+$
3.545	$\frac{5}{2}^+$	1.38±0.19	0.45±0.07[h]	1200±180	6.09±0.06	8.34	3.592	$\frac{5}{2}^+$
4.294	$\frac{5}{2}^+$	16.48±0.65	5.36±0.31	65.9±3.6	4.82±0.02	5.21	4.445	$\frac{5}{2}^+$
4.468	$\frac{3}{2}^+$	32.09±0.34	10.45±0.46	30.4±1.2	4.48±0.02	4.44	4.353	$\frac{3}{2}^+$
5.022	$(\frac{5}{2}^+,\frac{3}{2}^+)$	7.76±0.68	2.53±0.25	88±8	4.95±0.04	4.67	5.600	$\frac{3}{2}^+$
5.386		7.47±0.55	2.43±0.21	71±6	4.85±0.03	5.33	5.345	$\frac{7}{2}^+$
5.758		1.06±0.06	0.34±0.03	384±27	5.59±0.03	4.99	6.147	$\frac{7}{2}^+$
5.867		1.89±0.10	0.62±0.04	198±13	5.30±0.03	4.84	6.230	$\frac{3}{2}^+$
5.979		1.44±0.16	0.47±0.06	239±28	5.38±0.05	4.82	6.602	$\frac{7}{2}^+$
6.094		0.43±0.03	0.14±0.01	730±60	5.86±0.03	4.65	6.932	$\frac{5}{2}^+$
6.21		0.42±0.06	0.14±0.02	690±110	5.84±0.06	5.68	7.322	$\frac{7}{2}^+$
6.341		2.63±0.19	0.86±0.07	98±8	4.99±0.03	4.59	7.588	$\frac{3}{2}^+$
6.500		3.29±0.13	1.07±0.06	69.1±3.8	4.84±0.02	4.73	7.689	$\frac{5}{2}^+$
						4.24	8.261	$\frac{5}{2}^+$
8.301		0.94±0.07	0.31±0.03	40.2±3.3	4.60±0.03	3.81	8.672	$\frac{5}{2}^+$
8.417		0.55±0.07	0.18±0.02	59±8	4.77±0.05	4.67	8.685	$\frac{3}{2}^+$
8.816		3.65±0.36	1.19±0.13	5.4±0.6	3.73±0.04	5.93	8.861	$\frac{7}{2}^+$
8.970	$\frac{5}{2}^+, T=\frac{3}{2}$	8.56±0.33	2.79±0.16	1.80	3.26	3.26	8.993	$\frac{5}{2}^+, T=\frac{3}{2}$
$E_p=2.718$[i]		0.93±0.32	0.30±0.11					

[a] Energies of bound states (below 2.43 MeV) are taken from Ref. 17, while the remaining three levels below 5 MeV are discussed in Sec. III A of the text. The energies above 5 MeV are from the present work only.

[b] Spins and parities are from Ref. 17.

[c] The sum of the proton decays equals 91.0%, since there is a 9.0% proton "background" made up of decays too weak to analyze (see discussion in text).

[d] The branching ratios and ft values are calculated assuming complete isospin purity of the $T=\frac{3}{2}$ state (see text), and allowance has been made for the 0.25% γ-decay branch from this state.

[e] The ft values are calculated using a ^{21}Mg mass excess of 10.911±0.016 MeV (Ref. 7) and a half-life of 122.5±2.8 msec.

[f] These calculations are from Ref. 2. For the predicted $T=\frac{1}{2}$ states between 6–9 MeV, no general attempt was made to correlate these individual levels with our experimental results.

[g] These branching ratios were calculated from comparison to the mirror ^{21}F decay (Ref. 28).

[h] This value has been corrected for the $\Gamma_\gamma/\Gamma \sim 2.5\%$ (Ref. 16).

[i] This unassigned peak is discussed in the text. Only the decay energy is listed, since the level from which it originates is uncertain.

^{20}Ne(d,n) reactions. In addition the energy levels in the mirror ^{21}Ne nucleus have also been recently investigated,[23] and assignments of mirror levels up to 4.8 MeV have been made for these nuclei (cf. Refs. 17 and 23). It therefore seems reasonably unlikely that additional levels capable of being fed by allowed β decay could exist in this energy region. Further, it is unlikely that higher-lying levels would decay solely to excited states in ^{20}Ne and not to the ground state as well (although this clearly depends upon the exact nature of the wave functions).

The assignment of observed proton decay energies to levels in ^{21}Na generally follows the assumptions noted above. One exception to this can be seen in Table I. The decay of the 5.39-MeV state is shown leading only to the first excited state of ^{20}Ne; the ground-state branch was not observed. This decay energy was not assigned to an energy level in ^{21}Na decaying to the ^{20}Ne(g.s.), since to do so would have meant postulating a new level at ~3.75 MeV, where none now exists. Peak 10, on the other hand, was not assigned to any level in ^{21}Na, though it certainly arises from the β^+ decay of ^{21}Mg. However, it is not certain whether this relatively small peak is due to decay to the ground state, or the first excited state in ^{20}Ne. Though it was not assigned a parent state in ^{21}Na, the intensity is included in subsequent branching-ratio determinations.

Three peaks arise from the decay of the $T=\frac{3}{2}$ state (denoted by the vertical arrows in Figs. 2 and 3); the proton decay to the second excited state was not observed, although it would appear in the region of peak 8. This peak consistently exhibits a width three times larger than is observed for the other (isospin-forbidden) decays of the analog state.

Table I also shows the comparison of our deduced ^{21}Na energy levels with those found in the literature.[20,22] As noted in Sec. III A, proton groups 2, 5, and 6 shown in Table I were used as part of the energy calibration; the corresponding excitation energies in ^{21}Na result directly from the data of Refs. 15, 16, and 17. No comparison with these values is therefore shown under the heading "previous work." Additionally, only those energies are listed in the last three columns of Table I that reasonably correspond to the excitation energies deduced from our data.

Although some $T=\frac{1}{2}$ states above 5 MeV in ^{21}Na have been established, spin and parity assignments for these states are generally unavailable. As it is difficult to correlate our results with previous measurements, the energies of states above 5 MeV are taken from the present study, and are used for all subsequent calculations.

Relative intensities for all measurable proton decays of ^{21}Na were determined. The fraction of the total proton decays is listed in Table II for each level. While considerable effort was made to account for all possible proton decays, there was a small portion (~9%) of decays in the spectra apparently due to weakly populated, broad levels. This "background" was not attributable to multiply scattered β particles, and the half-life of the appropriate energy region of the spectrum in each case was consistent with the ^{21}Mg half-life.

B. Branching Ratios and logft Values

The relative proton intensities are directly related to the transition rate of the preceding positron decay, since the typical γ-decay widths are on the order of 10^2 to 10^3 times smaller than the proton decay widths.[16] Even for the isospin-forbidden proton decay of the $T=\frac{3}{2}$ state, Γ_γ is ~9 eV (using the results from Ref. 21 and our ratio of Γ_{p_0}/Γ), while Γ is 1200–1500 eV (Refs. 11 and 24). Absolute branching ratios for β^+ decay to these unbound levels can be obtained from the calculated β^+ transition strength to the analog state. Assuming complete isospin purity for the J^π, $T=\frac{5}{2}^+$, $\frac{3}{2}$ level in ^{21}Na, the ft value for this transition can be calculated[25]:

$$ft=\frac{2\pi^3(\ln 2)(\hbar^7/m_0{}^5c^4)}{g_V'^2\langle 1\rangle^2+g_A'^2\langle\sigma\rangle^2}\,. \tag{2}$$

Using recent values[26] for g_V' and g_A', the renormalized vector and axial-vector coupling constants, respectively, one obtains

$$ft=\frac{6.15\times 10^3}{\langle 1\rangle^2+1.50\langle\sigma\rangle^2}\ \text{sec}\,, \tag{3}$$

where $\langle 1\rangle$ represents the Fermi matrix element, and $\langle\sigma\rangle$ the Gamow-Teller matrix element. These matrix elements for a β^+ transition between an initial state $|\psi_i(J_iT_i)\rangle$ with spin and isospin (J_iT_i) and a final state $|\psi_f(J_fT_f)\rangle$ are given by

$$\langle 1\rangle=\langle\psi_f(J_fT_f)|\sum_n\tau_+(n)|\psi_i(J_iT_i)\rangle\,, \tag{4}$$

$$\langle\sigma\rangle=\langle\psi_f(J_fT_f)|\sum_n\sigma(n)\cdot\tau_+(n)|\psi_i(J_iT_i)\rangle\,, \tag{5}$$

where $\tau_+(n)$ is the isospin ladder operator which changes a proton into a neutron, $\sigma(n)$ is the Pauli spin operator, and the summation is over all n nucleons.

Since τ_+ operates only on the isospin projection T_z, clearly the Fermi matrix element is zero unless $J_f=J_i$, $T_f=T_i$. Then

$$\langle 1\rangle^2=T(T+1)-T_{zi}T_{zf}\,; \tag{6}$$

for ^{21}Mg$\rightarrow{}^{21}$Na ($T=\frac{3}{2}$ state), $\langle 1\rangle^2=3$ for perfect

isobaric analogs.

The evaluation of $\langle\sigma\rangle^2$, on the other hand, is model-dependent. Recent shell-model calculations[2] predict a value of $\langle\sigma\rangle^2 \sim 0.27$ for this superallowed decay, confirming earlier estimates of $\langle\sigma\rangle^2$ based on the Nilsson formalism.[27] From Eq. (3), uncertainties in this estimation of $\langle\sigma\rangle^2$, even of the order of 50%, would affect the transition strength by only ~5% and the subsequent logft by ~0.02.

Lanford and Wildenthal have calculated[2] a logft for the decay of ^{21}Mg to the $T = \frac{3}{2}$ level in ^{21}Na of 3.26. Based on this, absolute branching ratios and partial half-lives can be derived for β^+ decays to proton-emitting states. These branching ratios are shown in column 4 of Table II. Lack of β-decay data to bound states in ^{21}Na precludes a worthwhile discussion of isospin mixing in its analog state.

Intensity ratios for bound levels are taken from the mirror $^{21}\mathrm{F}\ \beta^-\ ^{21}$Ne decay,[28] and are renormalized to the total decay strength to these levels as deduced from the total proton intensity. The resulting branching ratios are also given in Table II. In addition to these three allowed β-decay transitions, Harris and Alburger[28] reported an upper limit for the negatron branch leading to the 2.790-MeV state in ^{21}Ne. Rolfs *et al.*[23] have subsequently reported $J^\pi = \frac{1}{2}^-$ for this state, consistent with its assigned mirror in ^{21}Na. Hence there is a level at 2.80 MeV in ^{21}Na potentially fed by first-for-

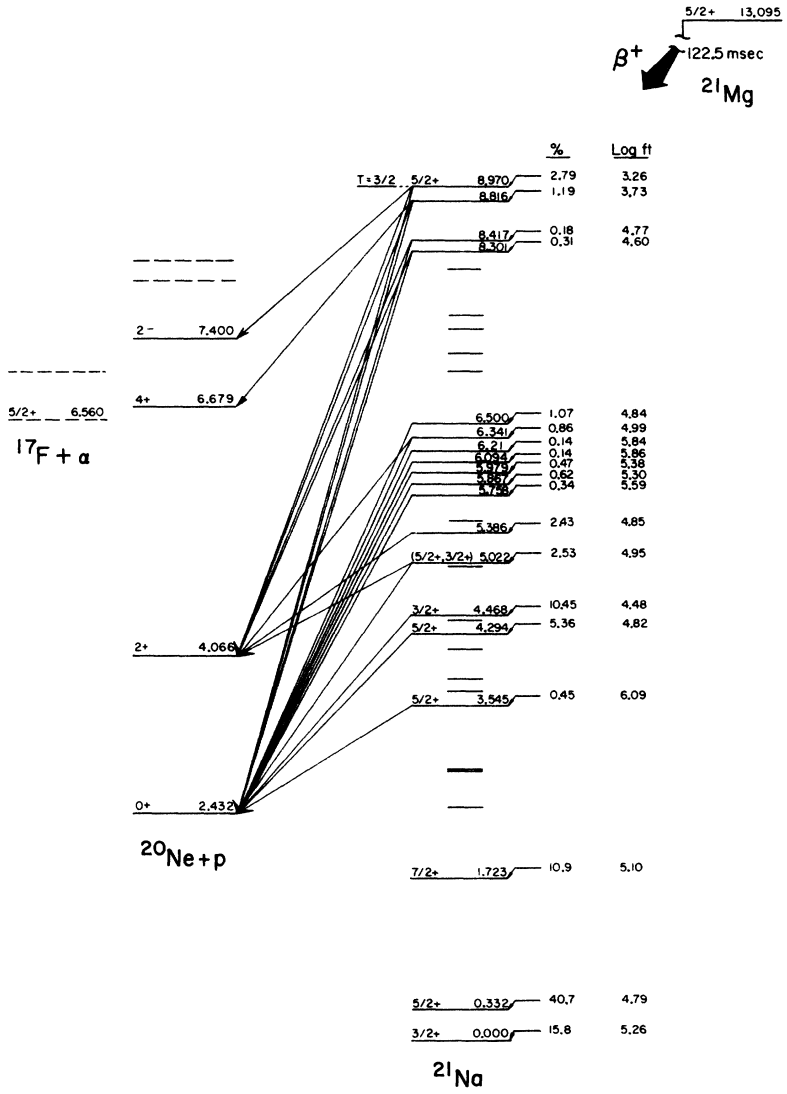

FIG. 6. Proposed decay scheme for ^{21}Mg. The excitation energies above 5 MeV in ^{21}Na are taken from this work (except the 8.970-MeV state). β^+-decay branching ratios and logft values are also indicated.

TABLE III. Energies, branching ratios, and penetrabilities for particle decays of the lowest $T=\frac{3}{2}$ state in ^{21}Na.

	Final[a] state (MeV)	J^π	Particle decay energy (c.m.) (MeV)	Observed[b] intensity I (%)	Relative branching ratio (%)	Penetrability[c] P	I/P
$p+^{20}$Ne	0.000	0^+	6.538	1.76 ± 0.12	20 ± 2	0.99	1.8
	1.634	2^+	4.904	4.78 ± 0.23	56 ± 3	1.57	3.0
	4.247	4^+	2.291	<0.35		0.061	<5.7
	4.968	2^-	1.573	2.02 ± 0.19	24 ± 2	0.096	21.0
	5.622	3^-	0.916	X		0.010	
	5.785	1^-	0.753	X		0.004	
$\alpha+^{17}$F	0.000	$\frac{5}{2}^+$	2.410	<1.60		0.070	<23
	0.495	$\frac{1}{2}^+$	1.915	X		0.002	

[a] Excited states in ^{20}Ne are from Ref. 18, while for ^{17}F they are from F. Ajzenberg-Selove, Nucl. Phys. A166, 1 (1971).

[b] These are stated in terms of the percent of the total proton decay of ^{21}Na. Possible groups marked X were unobserved, though within our range of observation. These results agree qualitatively with the observations in Ref. 11, where resonances were found in the p_0, p_1, and p_3 channels.

[c] This is calculated via

$$P=\frac{kR_0(A_1^{1/3}+A_2^{1/3})}{F_l^2+G_l^2},$$

where k depends on $\sqrt{E_{c.m.}}$; R_0 was chosen to be 1.3 fm and F_l^2 and G_l^2 are the regular and irregular solutions for the Coulomb wave equations evaluated for the lowest angular momentum transfer l.

bidden unique β decay. However, since only an upper limit for this decay has been established (i.e., a lower limit on the ft value), our calculations for the branching ratios ignore this possibility.

Statistical rate function, f, calculations were made for each positron decay shown in Table II, using the method of Bahcall.[29] These calculations correct for finite nuclear size and screening effects. In addition, the "outer" radiative corrections[30] were also made, though they are, given the above normalization to the analog state decay, extremely small. The decay scheme for ^{21}Mg is shown in Fig. 6 and includes branching ratios and logft values from this work.

Shell-model predictions for energy levels and β-decay transition strengths in mass 21 are taken from Lanford and Wildenthal,[2] and are shown in the last three columns of Table II. These calculations used a complete $0d$-$1s$ basis space for the five nucleons outside an ^{16}O core. Logft values were obtained for the $T=\frac{1}{2}$ levels of $J^\pi=\frac{3}{2}^+$, $\frac{5}{2}^+$, and $\frac{7}{2}^+$, as well as for the $T=\frac{3}{2}$ level (see additional discussion below).

The particle decays of the lowest $T=\frac{3}{2}$ state in ^{21}Na are shown in Table III. Of the decays not seen, penetrability calculations show that only proton decay to ^{20}Ne* (4.25 MeV) and α-decay to ^{17}F-(g.s.) might be expected. An upper limit for each of these two decays has been obtained, but neither is included in the branching-ratio and logft calculations (Table II). Intensities and reduced-width ratios are shown in Table IV for those $T=\frac{1}{2}$ states having more than one observed decay branch.

TABLE IV. Branching ratios and reduced widths for $T=\frac{1}{2}$ states in ^{21}Na.

E_x in ^{21}Na (MeV)	Intensity[a] of proton decay To g.s.	To 1×	To 2×	Intensity ratios 1×/g.s.	2×/g.s.	Ratio of reduced widths[b] 1×/g.s. $\frac{3}{2}^+,\frac{5}{2}^+$	$\frac{7}{2}^+$	2×/g.s. $\frac{3}{2}^+,\frac{5}{2}^+$	$\frac{7}{2}^+$
5.022	2.44 ± 0.64	5.32 ± 0.17		2.2		4.3	···		
6.341	1.15 ± 0.16	1.47 ± 0.13		1.3		0.73	0.11		
8.301	0.15 ± 0.02	0.79 ± 0.06		5.3		3.2	0.48		
8.417	0.23 ± 0.02	0.32 ± 0.06		1.4		0.85	0.13		
8.816	0.18 ± 0.03	0.80 ± 0.16	2.66 ± 0.32	4.4	14.8	2.8	0.46	310	1.6

[a] This is quoted as the percentage of the total proton decays from ^{21}Na.

[b] The reduced widths are calculated by dividing the observed intensity by the penetrability for the decay (using the lowest possible l) assuming the state has $J^\pi=\frac{3}{2}^+$, $\frac{5}{2}^+$, or $\frac{7}{2}^+$. The penetrabilities were evaluated using $R_0=1.3$ fm.

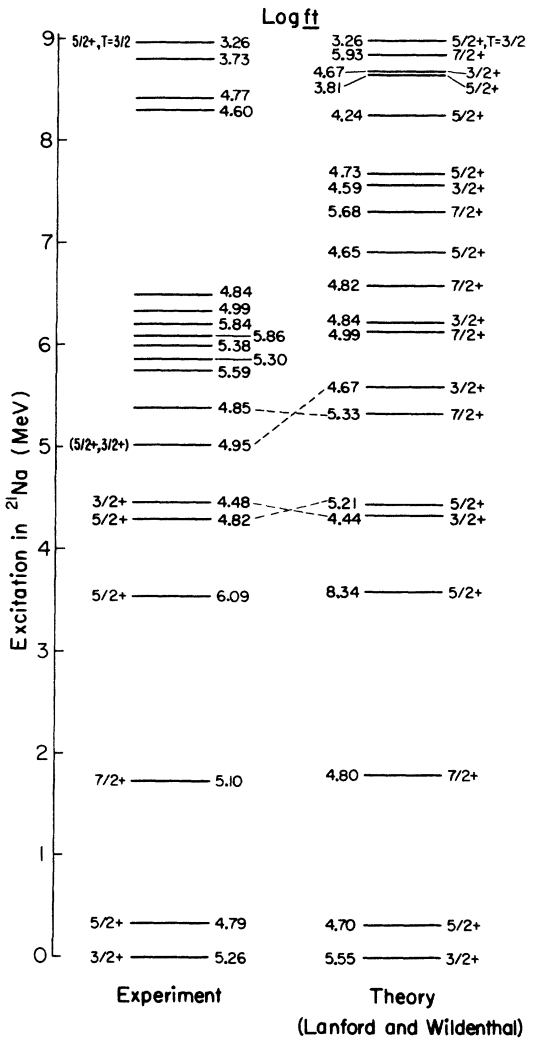

FIG. 7. Experimental and theoretical excitation energies and logft values for states in ^{21}Na fed by allowd β^+ decay of ^{21}Mg.

V. DISCUSSION AND CONCLUSIONS

The major experimental and theoretical results appearing in Table II have been illustrated in Fig. 7. Enough data exist to permit comparisons of theoretical and experimental β-decay transition rates to levels through 5.6 MeV in excitation. Such a comparison shows excellent agreement except for the decay to the 3.5-MeV state, for which a strongly hindered transition is predicted. Although our results indicate that this decay has a considerably greater strength than predicted, it is the weakest of all the (allowed) β-decay rates measured. Qualitatively the difference between experiment and theory for this case probably represents only a small change in the matrix-element cancellations arising from details of the wave functions.

Based on known spins and parities for states at 4.29 and 4.47 MeV, the predicted levels at 4.35 ($J^\pi = \frac{3}{2}^+$) and 4.45 MeV ($J^\pi = \frac{5}{2}^+$) have been inverted in order that the known and predicted spins correspond. The level at 5.022 MeV has been tentatively assigned $J^\pi = (\frac{5}{2}^+, \frac{3}{2}^+)$, based on earlier measurements.[17] The shell-model calculations show a state at 5.60 MeV with $J^\pi = \frac{3}{2}^+$, while the next available $\frac{5}{2}^+$ state is predicted to be at 6.9 MeV. Thus we have also inverted the theoretical levels at 5.35 and 5.60 MeV in Table II to align these possible $\frac{3}{2}^+$ states. (The alignment of these pairs of levels is shown in Fig. 7 by dashed lines.)

A more circumstantial case may be made for correlating our experimentally deduced level at 5.386 MeV with that calculated at 5.35 MeV. The measured and predicted transition rates show moderate agreement, and a state at 5.34 MeV has been identified by Butler *et al.*[20] in ^{23}Na(p, t). If this state has $J^\pi = \frac{7}{2}^+$, the two-neutron transfer could readily proceed via $L = 2$ pickup, while a ^{20}Ne(p, p) resonance experiment would require $l = 4$. This might explain why no level at this excitation has been previously reported from such resonance experiments.

Of the 16 $J^\pi = \frac{3}{2}^+, \frac{5}{2}^+, \frac{7}{2}^+$, $T = \frac{1}{2}$ levels predicted above the proton separation energy, 15 levels with logft values consistent with allowed Gamow-Teller decay were experimentally located, plus one additional unassigned decay that almost certainly belongs to a separate, though unidentifiable level. The sum of the predicted strengths to the first eight states in ^{21}Na (up through 5.6 MeV) is 90% of the total calculated decay strength from ^{21}Mg, while our experimental results indicate 89% of the total β^+-decay populates these states. Individual comparisons of the predicted and experimental transition strengths for decay to these low-lying levels show a difference of less than 10% between logft values (with the exception of the 3.5-MeV state noted previously). This reinforces the 5% (rms) and 12% (maximum) deviation in the *logarithm* found by Lanford and Wildenthal[2] in a more general study of theoretical vs experimental logft values in the mass ranges $A = 17-22$ and 35–39.

The level at 8.816 MeV has a relatively fast transition rate.[31] It should be emphasized that this strength is predicated on our assignment of peaks 7, 20, and 24 to this level which is the best assumption based on observed decay energies and widths. If one assumes that mixing between this level and the 8.970-MeV $T = \frac{3}{2}$ level (assuming identical J^π) might simply account for this enhanced decay strength, the necessary $T = \frac{3}{2}$ admixture can be estimated. However, the result-

ing admixture of ~30% would imply both an unusually strong charge-dependent matrix element and an isospin impurity of the $T=\frac{3}{2}$ state considerably greater than that experimentally determined for $T=\frac{3}{2}$ states in ^{17}F and ^{33}Cl (Ref. 1). Further, if such substantial mixing *were* to occur between these levels, one might expect the particle decay modes of these levels to be similar. Tables III and IV, and Fig. 6 show that this is not the case. Since Lanford and Wildenthal[2] in fact predict a logft of 3.81 for a $\frac{5}{2}^+$ state at 8.67 MeV (see Table II and Fig. 7) which compares remarkably well with the experimental logft of 3.73 for the 8.816-MeV level, our preferred explanation for this decay is to suggest the correspondence of these levels.

From our basic assumption of isospin purity for the lowest $T=\frac{3}{2}$ level in ^{21}Na, and the resulting β-decay transition rates to other levels in ^{21}Na, the expected half-life for the mirror β^- decay of ^{21}F can be estimated. The mirrors in ^{21}Na and ^{21}Ne have been assigned up to 5 MeV.[23] Hence the partial half-lives for allowed β^- decay to the first six levels with $J^\pi=\frac{3}{2}^+$, $\frac{5}{2}^+$, or $\frac{7}{2}^+$ in ^{21}Ne can be calculated from our experimental values of $(ft)^+$ for positron decay to analog levels in ^{21}Na. Comparison of this predicted half-life with the measured ^{21}F half-life of 4.35 ± 0.04 sec[32] gives $(ft)^+/(ft)^-=1.10\pm0.08$. This value of $(ft)^+/(ft)^-$ is consistent with the recent results for mass 17, where $(ft)^+/(ft)^-=1.151\pm0.033$ (Ref. 33). Other odd mass mirrors (i.e., $A=9, 13, 25$) also continue to show positive and significant values[34] of $\delta=[(ft)^+/(ft)^-]-1$. As discussed in a very recent analysis by Wilkinson *et al.*,[5] the possible origin of these asymmetries in the odd-A systems as due to lack of perfect analog symmetry in the final states should be studied.

ACKNOWLEDGMENT

We would like to thank W. A. Lanford and B. H. Wildenthal for several useful discussions regarding the logft calculations, and for supplying the additional predictions for ^{21}Mg β decay not listed in their publication.

†Work performed under the auspices of the U. S. Atomic Energy Commission.

[1]J. C. Hardy, J. E. Esterl, R. G. Sextro, and J. Cerny, Phys. Rev. C **3**, 700 (1971); a more general review of this topic appears in: J. C. Hardy, in Nuclear Spectroscopy and Reactions, edited by J. Cerny (Academic, New York, to be published).

[2]W. A. Lanford and B. H. Wildenthal, Phys. Rev. C **7**, 668 (1973); private communication.

[3]D. H. Wilkinson, Phys. Lett. **31B**, 447 (1970).

[4]J. C. Hardy and R. E. Bell, Can. J. Phys. **43**, 1671 (1965); R. E. Verrall, McGill University, Ph.D. thesis, 1968 (unpublished).

[5]D. H. Wilkinson, D. R. Goosman, D. E. Alburger, and R. E. Marrs, Phys. Rev. C **6**, 1664 (1972).

[6]R. D. Macfarlane, R. A. Gough, N. S. Oakey, and D. F. Torgerson, Nucl. Instrum. Methods **73**, 285 (1969).

[7]A. H. Wapstra and N. B. Gove, Nucl. Data **A9**, 265 (1971). These tables have been used for mass excesses throughout this paper, except as explicitly noted.

[8]D. H. Wilkinson, D. E. Alburger, D. R. Goosman, K. W. Jones, E. K. Warburton, G. T. Garvey, and R. L. Williams, Nucl. Phys. **A166**, 661 (1971).

[9]F. S. Goulding, D. A. Landis, J. Cerny, and R. H. Pehl, Nucl. Instrum. Methods **31**, 1 (1964).

[10]B. Teitelman and G. M. Temmer, Phys. Rev. **177**, 1656 (1969): ^{25}Al.

[11]A. B. McDonald, J. R. Patterson, and H. Winkler, Nucl. Phys. **A137**, 545 (1969): ^{21}Na.

[12]G. C. Morrison, D. H. Youngblood, R. C. Bearse, and R. E. Segel, Phys. Rev. **174**, 1366 (1968): ^{25}Al.

[13]W. Benenson, E. Kashy, and I. D. Proctor, Bull. Am. Phys. Soc. **17**, 891 (1972); Phys. Rev. C **7**, 1143 (1973).

[14]R. A. Gough, R. G. Sextro, and J. Cerny, Phys. Lett. **43B**, 33 (1973).

[15]C. van der Leun and W. L. Mouton, Physica **30**, 333 (1964).

[16]R. Bloch, T. Knellwolf, and R. E. Pixley, Nucl. Phys. **A123**, 129 (1969).

[17]F. X. Haas, C. H. Johnson, and J. K. Bair, Nucl. Phys. **A193**, 65 (1972).

[18]F. Ajzenberg-Selove, Nucl. Phys. **A190**, 1 (1972).

[19]D. F. Torgerson, K. Wien, Y. Fares, N. S. Oakey, R. D. Macfarlane, and W. A. Lanford, to be published .

[20]G. W. Butler, J. Cerny, S. W. Cosper, and R. L. McGrath, Phys. Rev. **166**, 1096 (1968).

[21]R. C. Bearse, J. C. Legg, G. C. Morrison, and R. E. Segel, Phys. Rev. C **1**, 608 (1970).

[22]P. M. Endt and C. van der Leun, Nucl. Phys. **A105**, 1 (1967).

[23]C. Rolfs, H. P. Trautvetter, E. Kuhlmann, and F. Riess, Nucl. Phys. **A189**, 641 (1972).

[24]G. M. Temmer, in *Nuclear Isospin*, edited by J. D. Anderson, S. D. Bloom, J. Cerny, and W. W. True (Academic, New York, 1969), p. 81.

[25]E. J. Konopinski and M. E. Rose, in *Alpha-, Beta-, and Gamma-Ray Spectroscopy*, edited by K. Siegbahn (North-Holland, Amsterdam, 1965), p. 1327.

[26]R. J. Blin-Stoyle and J. M. Freeman, Nucl. Phys. **A150**, 369 (1970), and references therein.

[27]J. C. Hardy and B. Margolis, Phys. Lett. **15**, 276 (1965).

[28]W. R. Harris and D. E. Alburger, Phys. Rev. C **1**, 180 (1970).

[29]J. N. Bahcall, Nucl. Phys. **75**, 10 (1966).

[30]D. H. Wilkinson and B. E. F. Macefield, Nucl. Phys. **A158**, 110 (1970).

[31]N. B. Gove, in *Nuclear Spin-Parity Assignments*, edited by N. B. Gove and R. L. Robinson (Academic, New York, 1966), p. 83.

[32]J. L. C. Ford, Jr., J. K. Bair, C. M. Jones, and H. B. Willard, Nucl. Phys. **63**, 588 (1965).

[33]D. E. Alburger and D. H. Wilkinson, Phys. Rev. C **6**, 2019 (1972).

[34]A recent general review appears in Phys. Today **24** (11), 18 (1971), and references therein.